SCIENTIFIC REPORTS

OPEN

SUBJECT AREAS:
SYNAPTIC TRANSMISSION
MODEL ORGANISMS
DROSOPHILA
DEVELOPMENTAL BIOLOGY

Received
20 June 2011

Accepted
14 July 2011

Published
28 July 2011

Correspondence and requests for materials should be addressed to H.R.S. (halyna.shcherbata@mpibpc.mpg.de)

Hyperthermic seizures and aberrant cellular homeostasis in *Drosophila* dystrophic muscles

April K. Marrone[1], Mariya M. Kucherenko[1], Robert Wiek[2], Martin C. Göpfert[2] & Halyna R. Shcherbata[1]

[1]Max Planck Gene Expression and Signaling Group, Max Planck Institute for Biophysical Chemistry, Am Fassberg 11, 37077, Göttingen, Germany, [2]Department of Cellular Neurobiology, Georg August University, Max Planck Institute for Experimental Medicine, Hermann Rein 3, 37075 Göttingen, Germany.

In humans, mutations in the Dystrophin Glycoprotein Complex (DGC) cause muscular dystrophies (MDs) that are associated with muscle loss, seizures and brain abnormalities leading to early death. Using *Drosophila* as a model to study MD we have found that loss of Dystrophin (Dys) during development leads to heat-sensitive abnormal muscle contractions that are repressed by mutations in Dys's binding partner, Dystroglycan (Dg). Hyperthermic seizures are independent from dystrophic muscle degeneration and rely on neurotransmission, which suggests involvement of the DGC in muscle-neuron communication. Additionally, reduction of the Ca^{2+} regulator, Calmodulin or Ca^{2+} channel blockage rescues the seizing phenotype, pointing to Ca^{2+} mis-regulation in dystrophic muscles. Also, Dys and Dg mutants have antagonistically abnormal cellular levels of ROS, suggesting that the DGC has a function in regulation of muscle cell homeostasis. These data show that muscles deficient for Dys are predisposed to hypercontraction that may result from abnormal neuromuscular junction signaling.

Muscular dystrophy (MD) patients have progressive muscle weakening and loss and so far no cure exists to treat these fatal disorders. Many forms of MDs are associated with abnormalities in the evolutionary conserved Dystrophin Glycoprotein Complex (DGC) that links the extracellular matrix (ECM) to the cytoskeleton[1]. Dystrophin (Dys) is the main component of the DGC required for muscle stability and is found at extrasynaptic and synaptic regions of muscle fibers where it is required for neuromuscular junction (NMJ) development[2]. Dys structurally links cytoskeletal actin to the ECM via the glycoprotein Dystroglycan (Dg), where Dys also binds several other proteins (two syntrophins, two dystrobrevins, and four sarcoglycans)[3–4]. Improper association between muscle and the surrounding basal lamina is found in a variety of MDs and cardiomyopathies[5–7].

The DGC has been also shown to play a role in cellular signaling processes that require Dg extracellular binding to Laminin. For example, G-protein binding to Syntrophin activates PI3K/Akt signaling in a manner that is dependent upon Laminin-Dg interaction[8], as well Syntrophin phosphorylation has been shown to be dependent upon this interaction resulting in Syntrophin-Grb2-Sos1-Rac1-Pak1-JNK signaling[9]. Additionally, the DGC is involved in TRPC channel activation at the muscle sarcolemma where Syntrophin regulates cation influx via anchoring the store-operated channels that are critical for normal calcium homeostasis in muscle cells[10–11].

Recently *Drosophila* has been shown to be a suitable genetic model to study the DGC[12]. Initial characterization of the DGC in *Drosophila* has portrayed that components studied so far are evolutionary conserved[13] and DGC deficiencies lead to age dependent muscle degeneration, reduced mobility, dilated cardiomyopathy and a shorter life span[12,14–15]. Using this *Drosophila* MD model we previously performed *in vivo* genetic screens in ageing dystrophic muscles to find novel DGC interactors[16]. These interactors were divided into three main functional groups: mechanosignaling, cellular stress response, and neuron-muscle communication. While the role of the DGC in providing muscle integrity has been extensively studied, its function in muscle-neuron communication has not been fully defined.

Since our previous data showed that the DGC mutants and the interactors found in the screen show mobility defects that are intensified by higher temperatures, we decided to analyze the reason for this behavioral defect. Temperature induced walking disability can originate from muscle or neuron malfunction. Here we measured the muscle activity on live dystrophic animals and showed that *Drosophila Dys* mutants have muscle defects resulting in seizures. These seizures robustly occur at elevated temperatures that seem to enhance an underlying

physiological defect. On further inspection we have determined that this phenotype is only displayed when Dys is downregulated during development of muscles, implying a developmental requirement for Dys. Surprisingly, the seizure phenotype is not shared by, and repressed by mutations in, the binding partner of Dys, Dg, possibly due to malfunctioning of the NMJ. In addition, we show that a deficiency in the Ca^{2+} regulator Calmodulin (Cam) and calcium channel blockers rescue the *Dys* phenotype, suggesting that Ca^{2+} plays a role in dystrophic seizures. Under stress *Dys* and *Dg* mutants have altered levels of ROS suggesting that these proteins play a role in maintaining cellular homeostasis. These results reveal novel dynamics between two components of the DGC and their interaction.

Results

In a previous report we showed that the DGC is involved in the stress response pathway and that energetic stress and changes in the ambient temperature accelerate dystrophic muscle degeneration[16]. Therefore we decided to test if dystrophic animals show abnormal cellular homeostasis. Since elevated temperatures enhance cellular responses[17–18], we measured the amount of lipid peroxidation products which are the result of reactive oxygen species (ROS) of animals kept for three days at 29°C (higher than ambient, but not heat shock temperature). *Dys* mutants had a strikingly larger amount of lipid peroxidation products than did *wt* animals (Fig. 1a). Inversely, *Dg* mutants have significantly decreased ROS levels relative to control. Though heterozygous single mutants (*Dys*/+ and *Dg*/+) do not have

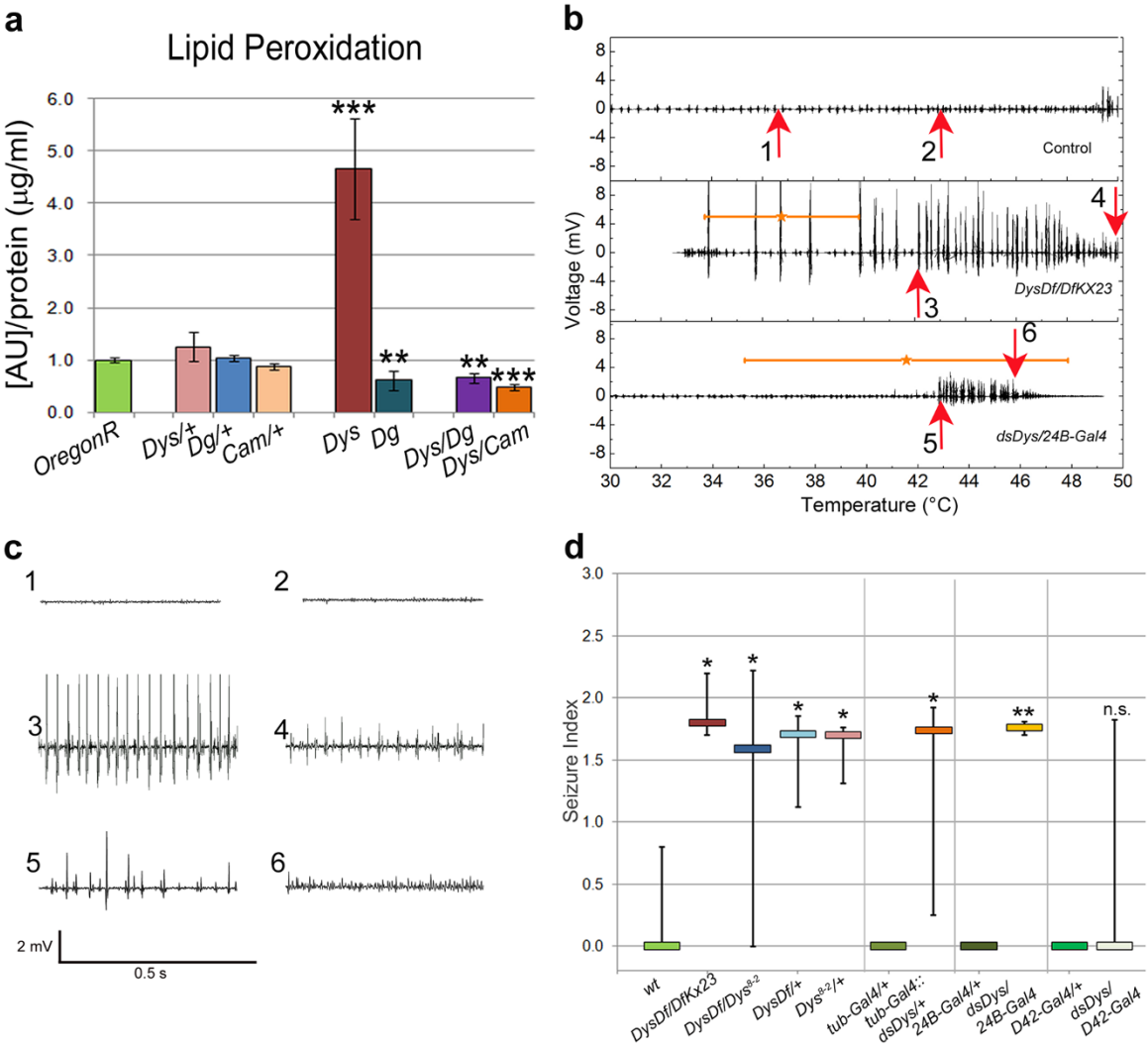

Figure 1 | *Dystrophin* mutants have elevated ROS and hyperthermic seizures. (a) Assessment of cellular lipid peroxidation products normalized to protein content in animals housed at 29°C for three days. The axis represents the raw molar absorption after blank subtraction and normalization to protein content. Statistical analysis was done using a one-tailed Student's t-test and the error bars represent the standard deviation. All comparisons are made against *OregonR*. Exact experimental values and P-values are given in Supplementary Table 1. (b) Electrical output from IFM vs. temperature during seizures of *DysDf/DfKX23* and *dsDys/24B-Gal4* mutants compared to Control. Stars indicate the average start temperature where the error bar indicates the standard deviation. Arrows indicate where plots in panel c are taken from. (c) Electrical output relative to time where the region examined correlates with the numbered arrows in panel b. Output is displayed over a 0.5 s time period emphasizing the increase in frequency and decrease in amplitude as the seizure progresses. (d) All tested *Dys* classical and *RNAi* alleles (levels of *Dys* mRNA downregulation are shown in Supplementary Table 2) had hyperthermic seizures with similar seizure indices tested in a two-tailed Kruskal-Wallis test where P=0.316 excluding data from *dsDys/D42-Gal4* animals (Supplementary Figure 1, Table 1). Seizure indices of dystrophic mutants are significantly higher when compared to the appropriate control (separated by vertical lines). One to one comparative statistics were done using a one-tailed Mann-Whitney U-test. Error bars indicate the 25th and 75th percentiles of the data spread considering that if an animal does not seize then the index is 0. The S_i range of some controls have zero values in the 25th and 75th percentile range, thus it appears that there is no error bar.*P ≤ 0.05, **P ≤ 0.01, ***P ≤ 0.001.

changed ROS levels, the levels are significantly decreased in double heterozygous mutants (*Dg*/+; *Dys*/+) indicating that these two proteins interact in maintaining proper ROS cellular levels (Fig. 1a).

Cellular homeostasis depends on Ca^{2+} levels and a protein regulating proper calcium levels, Calmodulin (Cam) was found to interact with Dys leading to muscle degeneration[16]. We analyzed ROS levels of animals heterozygous for both *Cam* and *Dys* (*Cam*/+; *Dys*/+) and observed a significant decrease in ROS levels indicating that these two proteins genetically interact (Fig. 1a), suggesting that Dys-dependent cellular stress depends on Ca^{2+} levels.

Next, we applied higher than ambient temperatures to *Dys* classical and *RNAi* mutants to examine *in vivo* dystrophic muscle function in increased temperature conditions. This revealed a complex physiological defect that can be measured by electrophysiological recordings from indirect flight muscles (IFMs). All *Dys* mutant animals at temperatures ranging anywhere from 30–46°C started to have abnormal muscle contractions (seizures) (Fig. 1b–d, Supplementary Fig. 1). These seizures slowly decreased in amplitude while increasing in frequency. When a seizure occurred a seizure index (S_i) was calculated taking into consideration the amplitude and duration of the seizure as well as the temperature seizing started at. If an animal did not have a seizure then the S_i was assigned a value of zero (Table 1). Using different *Dys* allelic combinations we observed that 60–100% of dystrophic animals had seizures with the median S_i ranging from 1.6 to 2.4, while the median S_i for control animals was 0 (Table 1).

To understand the origin of this phenotype, we downregulated *Dys* in different tissues using specific *Gal4* drivers and *Dys RNAi*. Animals with ubiquitous and mesodermal *Dys* downregulation showed a strikingly similar phenotype to that seen with the allelic mutations (Fig. 1b,d). Contrarily, the indices were not significantly greater compared to control when *Dys RNAi* was expressed using a

Table 1 | Seizure Indices (S_i)

Genotype	n	% seized[Ŧ]	Avg. $T_s \pm$sd (°C)*	Avg. $A_{max} \pm$sd (mV)*	Avg. Area $\pm$sd (pixel $\times 10^{-3}$)*	Median S_i** ($25^{th}/75^{th}$ percentiles)	[+]P-value
OregonR	7	29	40.7±6.1	12.2±13.4	2.9 ± 2.4	0.0 (0.0/0.9)	0.944
w^{1118};*CyO*/+; *TM6*/+	4	25	46.4	2.6	1.3	0.0 (0.0/0.4)	($\chi^2 = 0.115$)
w^{1118};*CyO*/*Pin*	4	25	38.3	14.3	6.9	0.0 (0.0/0.6)	
*wt****	15	24	42.1±4.1	14.0±13.8	4.5±2.9	0.0 (0.0/0.8)	-
DysDf/*DfKX23*	5	80	37.0±3.1	6.0±5.2	2.4 ± 2.0	**1.8 (1.7/2.2)**	**0.028***
DfKX23/+	4	100	43.0±3.3	11±6.8	4.9 ± 5.4	**1.8 (1.5/2.2)**	**0.011***
DysDf/$Dys^{8\text{-}2}$	10	60	40.8±6.4	13±6.4	4.2 ± 2.9	**1.6 (0.0/2.2)**	**0.045***
$Dys^{8\text{-}2}$/+	5	80	40.2±8.2	3.3±1.7	1.4 ± 0.8	**1.7 (1.3/1.8)**	**0.045***
DysDf	9	89	35.2±4.7	7.7±6.4	4.9 ± 3.7	**2.4 (2.2/2.4)**	**2.6×10^{-4}*****
DysDf/+	8	75	39.6±3.5	8.7±5.3	2.4 ± 2.5	**1.7 (1.1/1.8)**	**0.050***
[◇]$Dg^{-/-}$	9	11	45.3	5.6	1.3	0.0 (0.0/0.0)	0.19
Dg^{O86}/+;*DysDf*/+	10	20	38.0±7.6	5.2±2.9	2.8 ± 0.3	0.0 (0.0/0.0)	0.50
[•]$para^{ts1}$/+; *DysDf*/+	5	0	0	0	-	-	0.28
$cora^{k08713}$	8	0	-	-	-	-	0.15
$cora^{k08713}$/+; *DysDf*/+	8	12.5	36.0°C	5.2	5.6	0.0 (0.0/0.0)	0.41
[•]Cam^{n339}/+; *DysDf*/+	7	0	-	-	-	-	0.19
tub-Gal4/+	10	20	42.5±5.5	2.6±0.1	1.6±0.4	0.0 (0.0/0.0)	-
tub-Gal4::dsDys/+	10	70	40.1±5.8	4.5±2.1	2.3 ±1.8	**1.7 (0.2/1.9)**	**0.020***
tub-Gal4::dsDg/+	8	50	43.6±2.6	4.1±2.1	1.2 ±0.7	0.7 (0.0/1.6)	0.19
tub-Gal4::dsDys/dsDg [£]	6	50	44.2±5.3	12±13.4	0.8 ±0.2	0.7 (0.0/1.4)	0.29
tub-Gal80^{ts}/+, *tub-Gal4::dsDys*/+ – Put to 29°C after eclosion	14	29	45.7±2.4	10±5.8	2.1 ± 1.2	0.0 (0.0/0.9)	0.47
tub-Gal80^{ts}/+, *tub-Gal4::dsDys*/+ – Put to 29°C as L3 larvae	13	77	40.1±4.9	7.9±5.2	4.2 ± 4.2	**2.0 (1.7/2.2)**	**3.7×10^{-4}*****
tub-Gal80^{ts}/+, *tub-Gal4::dsDg*/+ – Put to 29°C after eclosion	5	0	-	-	-	-	0.40
tub-Gal80^{ts}/+, *tub-Gal4::dsDys/dsDg* – Put to 29°C after eclosion	6	17	48.2	5.1	0.4	0.0 (0.0/0.0)	0.34
$para^{ts1}$/+; *tub-Gal4::dsDys*/+	5	0	0	0	-	-	0.40
CyO(Pin)/+;*24B-Gal4*/+	4	0	-	-	-	-	-
dsDys/*24B-Gal4*	5	100	41.5±6.3	5.8±4.1	3.1 ± 2.7	**1.8 (1.7/1.8)**	**0.0079****
dsDg/*24B-Gal4*	5	0	-	-	-	-	1.0
D42-Gal4/+	4	0	-	-	-	-	-
dsDys/*D42-Gal4*	5	40	37.8±8.2	5.7±5.2	2.3 ± 0.8	0.0 (0.0/1.8)	0.28
dsDg/*D42-Gal4*	5	0	-	-	-	-	1.0

n = number of animals measured for the specified genotype
[Ŧ]percent of animals measured that had a seizure
*Calculated using data from animals that seized only
**Index calculated by integrating the area of the graph of voltage vs. temperature during a seizure, taking the natural logarithm of this number, dividing by the temperature that the seizure started, and then multiplying times ten. A S_i of zero was assigned to animals that did not seize
***There is no difference between animals of genotypes *OregonR*, w^{1118};*CyO*/+;*TM6*/+ or w^{1118};*CyO*/*Pin* as assessed using a Kruskal-Wallis test. These animals were pooled and termed *WT*.
[+]P-values are relative to the control animals at the beginning of each shaded section, *P ≤ 0.05, **P ≤ 0.01, ***P ≤ 0.001
[◇]Five animals were of genotype $Dg^{O86/O55}$, two were of genotype Dg^{O86} and two were of genotype Dg^{O86}/+ where one animal of genotype $Dg^{O86/O55}$ had a seizure
[£]Four animals were of genotype *tub-Gal4::dsDg/dsDys* and two animals were of genotype *tub-Gal4::dsDys/dsDg*
[•]Animals of genotype $para^{ts1}$/*Y* and Cam^{n339}/+ did not have seizures (n=2)

motoneuron driver (Fig. 1d). From these data we conclude that seizures are a result of the lack of Dys in muscle tissue, but not in motoneurons.

The occurrence of temperature-sensitive seizures could be due to a problem arising upon Dys deficiency during muscle establishment or maintenance. To allow for developmental stage-specific downregulation of Dys, *RNAi* transgenic constructs were combined with the *Gal80* temperature-sensitive system that suppresses expression of constructs until the animals are transferred to 29°C. When *Dys RNAi* animals were shifted to 29°C after muscle development and synapse maturation is completed, a significant decrease in seizure indices took place compared to a Dys deficit in development (Fig. 2a,b). This evidence shows that Dys is required during development to prevent heat induced seizures.

Animals expressing *Dys RNAi* during development have properly developed muscles, which degenerate only as the animal ages[12]. To determine if previously shown age-dependent muscle degeneration is a result of the seizure activity described here, *Dys RNAi* animals were allowed to develop at a permissive temperature (no *RNAi* expression) and aged at the restrictive temperature after adult muscle and NMJ formation. Although the animals no longer had seizures, they exhibited muscle degeneration similar to animals with temporally unrestricted *Dys* downregulation (Fig. 2c,d, Supplementary Table 4). Importantly, seizing is not the result of aging since *wt* older animals still do not seize and older *Dys* mutants have a reduced occurrence of seizures (~50%). Perhaps, degenerating muscle is unable to respond in the same manner as young intact muscle. This result implies that the absence of Dys influences muscle degeneration and seizures independently.

The seizures in *Dys* mutants could be due to either muscle autonomous mis-regulation or inability to properly respond to synaptic input. To test if a neuronal contribution is required we used a previously described temperature-sensitive mutation in the *paralytic* gene that abolishes neuronal action potentials at temperatures above 29°C in adults (Fig. 2e)[19–20]. Opposite to *Dys* heterozygous and *RNAi* mutants, the introduction of the *para*^{ts1} allele into a dystrophic background prevented seizures suggesting that neuronal transmission is required to trigger contractions in dystrophic muscles.

We initially believed that mutations in Dys's binding partner, *Dg* would phenocopy the dystrophic seizure phenotype. Surprisingly, *Dg* loss-of-function mutants exhibit no seizing activity (Fig. 3a,b, Table 1). Ubiquitous *Dg RNAi* expression produced some small low occurrence seizures, but specific expression in the mesoderm and motoneurons caused no seizures (Supplementary Fig. 3). Even more, *Dg/+;Dys/+* transheterozygous animals did not have heat-induced contractions (Fig. 3a,b, Table 1). This reveals that seizure susceptibility at high temperatures can be reduced by loss of one copy of *Dg*.

It has been shown that at *Drosophila* larval NMJs Dys is not localized in the absence of Dg, while Dg localization is only partially dependent upon Dys[20]. Accordingly, we found that at adult dystrophic NMJs Dg is reduced (Fig. 3c,d), while in transheterozygous mutants (*Dg/+;Dys/+*) Dg is missing from the NMJ similar to *Dg* loss-of-function mutants (Fig. 3c,d, Supplementary Table 5). Based on this evidence, we propose that the presence of Dg at the NMJ is necessary for *Dys* mutants to have temperature-induced seizures. This conclusion is further supported by the fact that animals expressing both *Dg* and *Dys RNAi* (causing Dys and Dg levels to be reduced but not abolished, Supplementary Table 1,6) have lower seizure occurrence than *Dys RNAi* mutants (Table 1).

Since Dys and Dg are the key components of the DGC, integrity of which is crucial for proper muscle function and maintenance, we

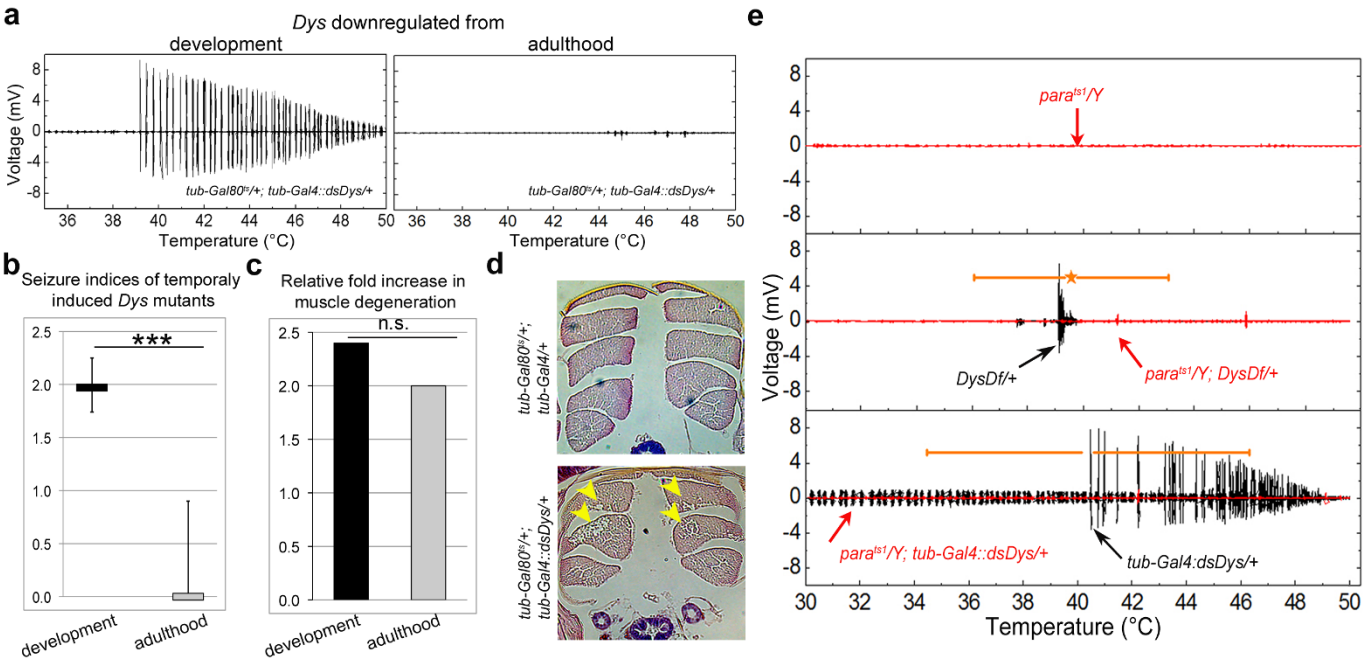

Figure 2 | Dystrophic seizures are dependent upon neuronal input that require Dys during development. (a) Electrical output of animals shifted to the restrictive temperature as late L3 larvae (left) and as adults (right). Dys protein reduction levels using the *Gal80* temperature sensitive system are given in Supplementary Table 3 and Supplementary Figure 2. (b) Seizure indices for *RNAi* mutants after being shifted to the restrictive temperature at different life stages. A Mann-Whitney U-test was used to compare seizure indices upon *Dys* downregulation in adulthood to *Dys* downregulation in development ($P = 0.007$). *Dys* downregulation in adulthood resulted in a S_i that is not significantly different from control (*tub-Gal4/+*, $P = 0.47$, Table 1). In addition, animals of the genotype *tub-Gal80*^{ts}*/+;tub-Gal4/+* shifted as adults did not have seizures ($n = 2$). (c) Bar graphs showing relative fold increase in the frequency of muscle degeneration of *Dys RNAi* mutants targeting *Dys* throughout the lifetime or shifted to the restrictive temperature as adult. The percent of muscle degeneration has been normalized to that in control animals under the same conditions (Supplementary Table 4). Statistics for muscle degeneration were done using a one-tailed chi-square test ($\chi^2=2.62$, $P = 0.11$). (d) Histological sections of thoracic muscles. Arrows indicate areas of degeneration. (e) The *para*^{ts1} allele abolishes seizures in *DysDf/+* and *tub-Gal4::dsDys/+* animals (red plot). *P ≤ 0.05, **P ≤ 0.01, ***P ≤ 0.001.

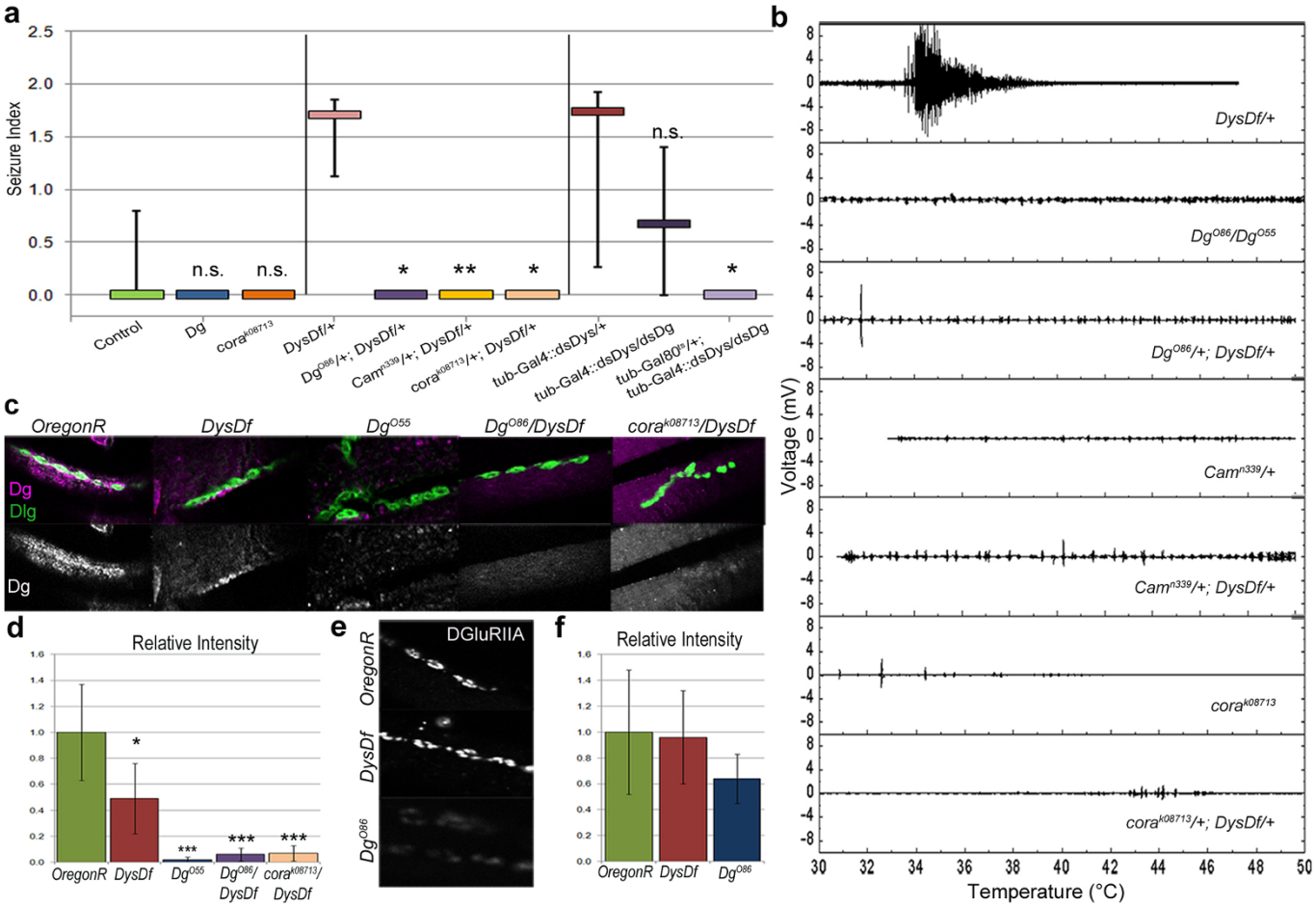

Figure 3 | Loss of Dystroglycan, Coracle or Calmoduline represses the seizure phenotype of *Dystrophin* mutants. (a) Seizure indices show that *Dg* and *cora* mutants do not have seizures (Table 1) and mutations in *Dg*, *Cam* or *cora* suppress the seizure phenotype in *Dys* transheterozygous animals ($P = 0.032$, 0.006 and 0.017 respectively when compared to *Dys*/+ animals). Animals carrying *RNAi* constructs against both *Dys* and *Dg* also showed a 50% decrease in seizure activity when downregulated during development and 17% when downregulated after development indicating a repression of the phenotype by downregulation of Dg ($P = 0.072$ and 0.017 respectively compared to *Dys RNAi* mutant, Table 1). Statistics were done using a one-tailed Mann-Whitney U-test. (b) Electrical output from IFM vs. temperature. (c) In control animals Dg (magenta) is localized to the NMJ. *Dys* mutants have a decreased amount of Dg at the NMJ, but some Dg localization is still observed. *Dg* mutants have no Dg localized to the NMJ. Transheterozygous animals (*Dg*/+;*Dys*/+, *cora*/+;*Dys*/+) show a significant decrease in Dg staining at the NMJ as well. The overall structure and presence of NMJs does not appear to be altered in the mutants as can be seen via Dlg staining (green). (d) In adult abdominal NMJs DGluRIIA is localized similarly in *Dys* mutants as in the wild type (*OregonR*) animals; however, *Dg* loss-of-function mutants have a decreased amount of the receptor. Statistics on relative intensities were done using a Student's t-test compared to *OregonR* where the error bars represent the average deviation from the mean. *$P \leq 0.05$, **$P \leq 0.01$, ***$P \leq 0.001$.

wanted to understand why *Dg* mutants do not have seizures while *Dys* mutants do. First, we considered that *Dg* mutants do not have temperature-sensitive seizures due to compensatory mechanisms. Integrins are likely candidates, as alpha (7B) integrin has been shown to compensate for Dg absence in mediating cell-extracellular matrix attachment[21]. If integrins are making up for loss of Dg, then trans-heterozygous animals might have enhanced seizures. However, the reduction of both *integrin* and *Dg* (mys^1/+;*Dg*/+) leads to a similar phenotype as mys^1/+ heterozygous animals, indicating that there is no genetic interaction between these two proteins in seizure occurrence (Supplementary Fig. 4).

Drosophila NMJs are glutamatergic, and previously it has been shown that Dg is required for proper localization of postsynaptic glutamate receptors at larval NMJs[20,22]. Since the amount of glutamate receptors influences muscle-neuron communications, we next analyzed the localization of glutamate receptor type II A (DGlulRIIA) at the adult NMJ. We found that *Dg* mutants have an approximately 40% decrease in the levels of the glutamate receptor at the NMJ (Fig. 3e,f). Conversely, this receptor in *Dys* mutants is localized like in *wt* animals (Fig. 3e,f) which is in accordance with previous reports on larvae[20,23]. This indicates that the seizing phenotype observed in *Dys* mutants is not due to mislocalization of DGlulRIIA.

Next, in order to analyze if the rescue of the seizing phenotype observed in *Dys*/+;*Dg*/+ transheterozygous mutants is due to interaction of Dys and Dg at the NMJ we used mutants of Coracle (Cora), a protein that is localized to the NMJ. Cora is the *Drosophila* homologue of mammalian brain 4.1 proteins[20] and it has been shown that Cora and Dg protein concentration at the NMJ are co-dependent[20]. Since in *cora*/+;*Dys*/+ mutants Dg is not properly localized to the adult NMJ (Fig. 3c,d), it would be expected that *cora* mutants should behave the same as *Dg* mutants and rescue dystrophic hyperthermic seizures, if they depend on DGC function at NMJs. Hypomorphic *cora* mutant animals exhibit a mild heat-induced muscle contraction phenotype of their own (Fig. 4a,b), but this activity is not of the nature described here, therefore no seizure indices were calculated for these animals. Data derived from *Dys* and *cora* transheterozygous animals (*cora*/+;*Dys*/+) mimicked that of the *cora* mutants and, similar to Dg reduction, rescued dystrophic seizures (Fig. 3a,b). Based on these data and previous reports of increased neurotransmitter release at dystrophic larval NMJs[23–24],

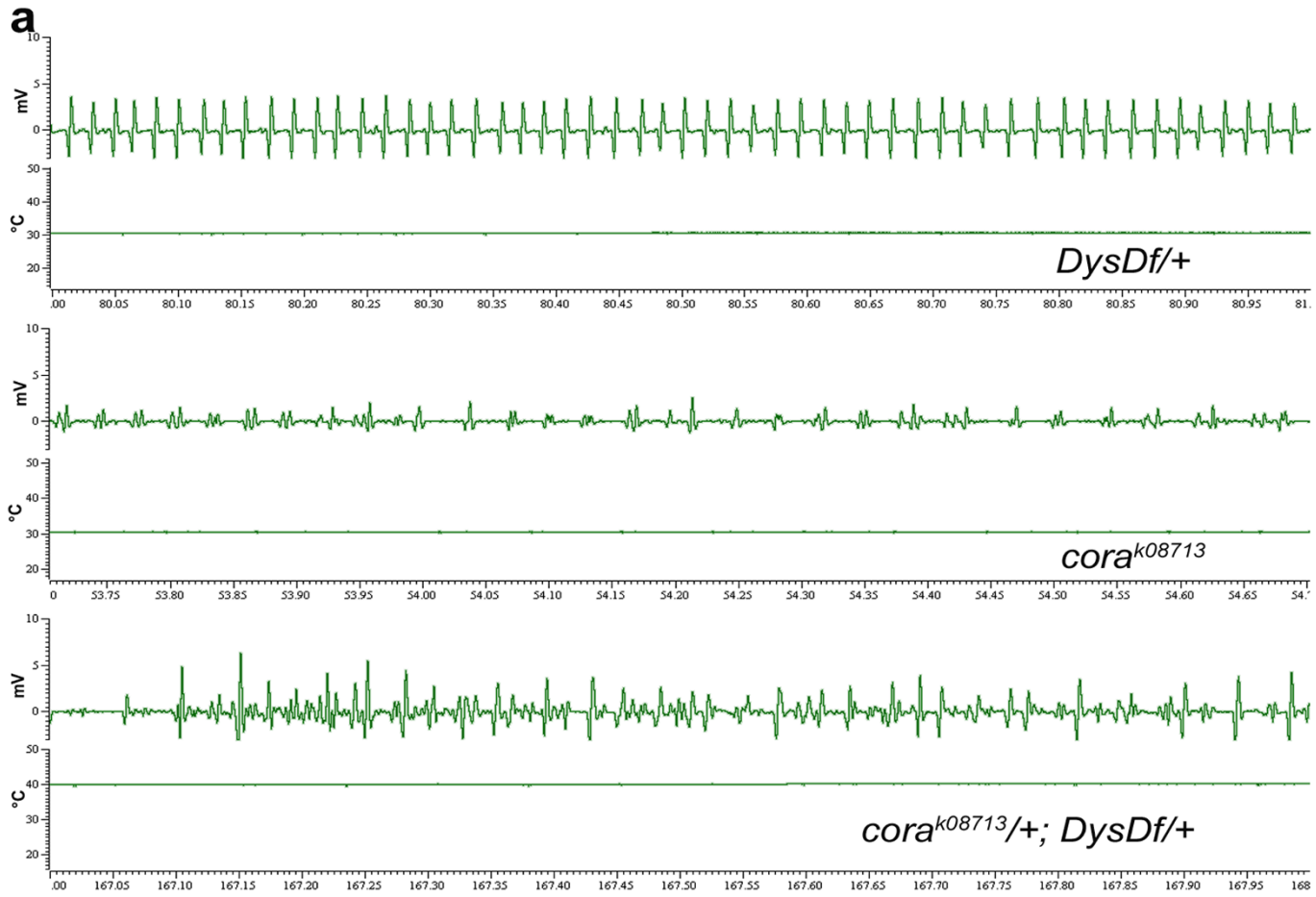

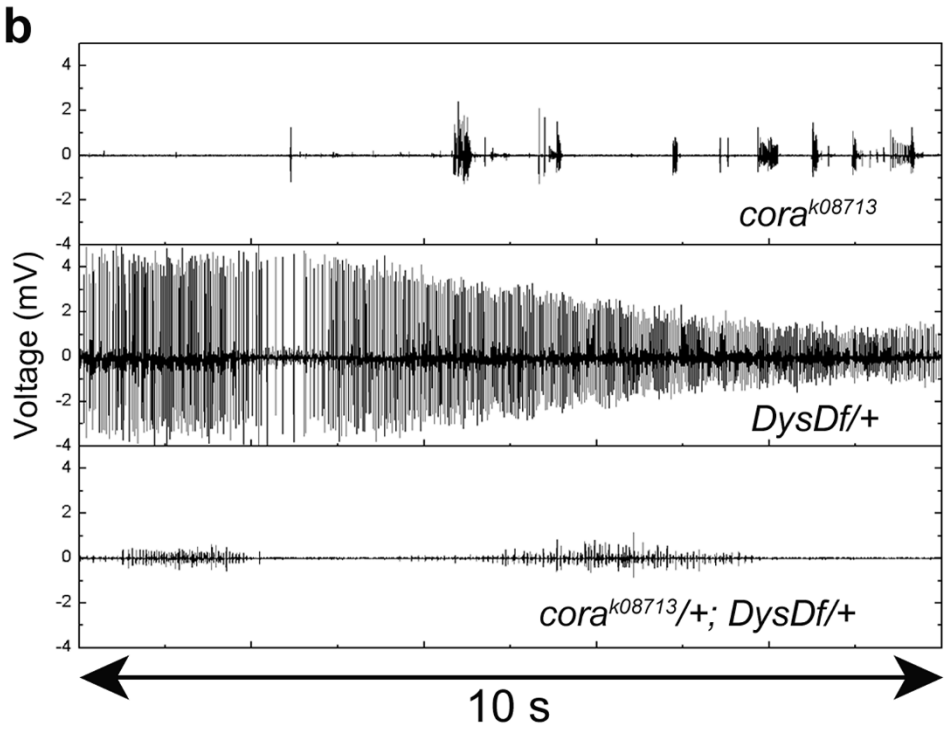

Figure 4 | ***Cora*** **mutants have a mild seizure phenotype that does not look like and overrides the dystrophic phenotype.** Mutation in the *cora* gene results in a distinctive electrophysiological phenotype from that seen with *Dys* heterozygous mutations. (a) *cora*^{k08713} mutants have electrical output that is not of a consistent frequency. Animals of genotype *cora*^{k08713}/+; *DysDf*/+ have a phenotype similar to the *cora* mutant. The output is recorded over 1 second. (b) Examples of the two types of electrical activity measured in *cora*^{k08713}, *DysDf*/+ and *cora*^{k08713}/+; *DysDf*/+ animals. The output is recorded over 10 seconds.

we suggest that hyperthermic seizures are derived from the improper function of the DGC at the NMJ.

Release of neurotransmitter at the NMJ results in depolarization of the muscle membrane causing release of Ca^{2+} from the SR required for muscle contraction. Thus, we examined how the Ca^{2+} binding protein, Calmodulin, which binds to DGC components dystrophin and syntrophins in mammals[25], affects the dystrophic seizure phenotype. In *Drosophila* there is only one gene encoding Cam that is homologous to the human CAM2 gene with 97% identity[26]. Introduction of a *Cam* null mutation into a *Dys* mutant background (*Cam*/+;*Dys*/+) rescued hyperthermic seizures (Fig. 3a,b). Since Cam regulates levels of Ca^{2+}, our data implies that Ca^{2+} levels are important for the dystrophic seizure activity.

Previous work has demonstrated that there is an increase in Ca^{2+} release from the sarcoplasmic reticulum (SR) in DMD human myotubes[27]. To assess by which mechanism Ca^{2+} plays a role in the observed seizures, *Dys* mutants were fed overnight various Ca^{2+} channel blockers [Nifedipine (dihydropyridine channel), 2-APB (inositol 1,4,5-triphosphate receptors, IP_3R) and Ryanodine (Ryanodine receptors, RyR)] and assayed for temperature induced seizures. To prevent total inhibition of muscle contraction a low drug concentration was used to block individual channels at one time. Animals fed Nifedipine did not show less seizure activity than controls, but both 2-APB and Ryanodine treated flies showed a decrease in seizure activity, with Ryanodine having the most dramatic effect (Fig. 5a,b, Supplementary Table 7). This shows that Ca^{2+} released via IP_3R and RyR activated channels plays a role in hyperthermic seizures.

Discussion

Muscle seizures accompany multiple human neurological and muscular disorders. Seizures can occur when a group of neurons becomes hyperexcited and discharge action potentials irregularly without suppression, which causes muscle fibers to contract inappropriately. The uncontrolled action potential is dependent upon K^+ and Na^+ channel permeability or Ca^{2+} mis-regulation[28]. Ryanodine receptors that are regulators of fast Ca^{2+} release from the sarcoplasmic reticulum have been found to play a role in the disease pathology of seizures[29]. Additionally, inositol 1,4,5-triphosphate receptors (IP_3Rs) which regulate slow Ca^{2+} release from the SR are necessary in the central nervous system, causing epilepsy when mutated[30]. Seizures can be alleviated by manipulation of ion channels or by blocking neurotransmission.

It has been shown that Laminin binds directly to voltage gated Ca^{2+} channels (Ca_V) at the presynapse in mice, specifically P/Q- and N-type channels, and this binding induces vesicle clustering[31]. Laminin also binds the transmembrane protein Dg providing a direct link between Dys and the presynaptic motoneuron in mammals. Importantly, not only does the motoneuron send signals to the muscle, but also retrograde signaling exists, where a signal travels from the muscle back to the presynaptic neuron. The current pathway by which synaptic retrograde signaling communicates is not known, however Dys has been implicated previously to play a role in the process[23–24]. If we assume that hyperthermic seizures reported here are related to the role of Dys in retrograde signaling, then the Ca_V-Laminin-Dg signaling cascade could explain why the P/Q- and N-type, but not the L-type Ca^{2+} channel blocker affected *Dys* seizures. Similarly, the reduction of Dg or Cora reduced the seizure occurrence possibly by preventing propagation of signaling via loss of communication with Laminin. Another pathway that plays a role in retrograde signaling at the NMJ[32] is TGF-β and interestingly, mutants of the TGF-β pathway have a hyperthermic seizure phenotype similar to *Dys* mutants (Supplementary Fig. 5). However, we did not observe a genetic interaction between the DGC and TGF-β pathway components suggesting that they might act in parallel.

Dys and Dg have been reported to have opposing functions in control of neurotransmitter release at the NMJ. *Dg* mutants show a decrease and *Dys* loss of function and heterozygous mutants an increase in release of neurotransmitter, however both mutants do not show a change in response to altered neurotransmitter levels[20,22–24].

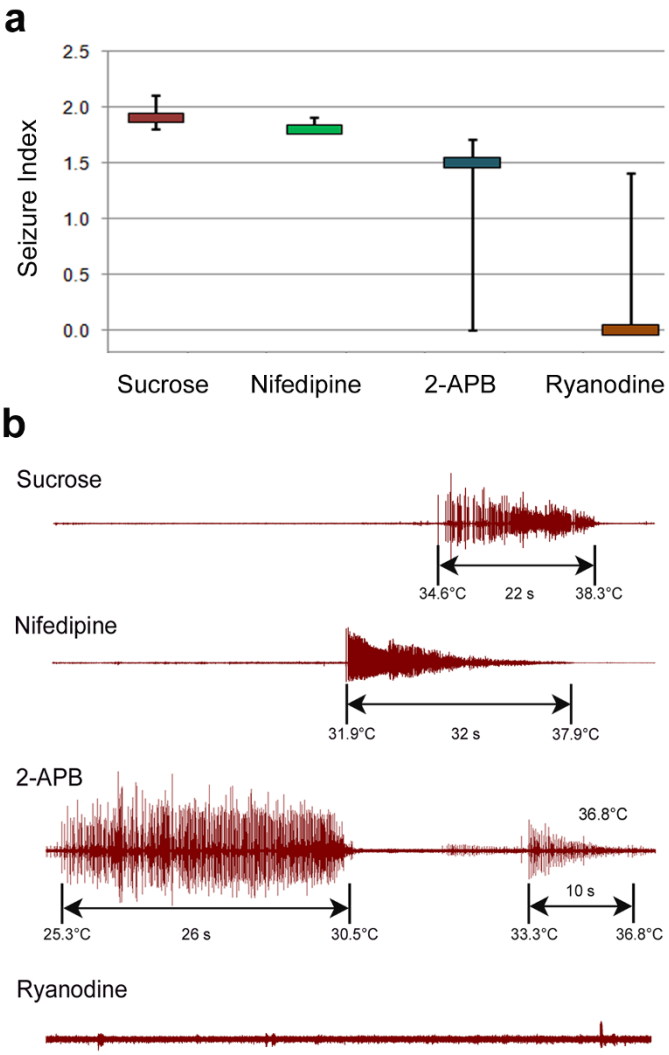

Figure 5 | Elevated Ca^{2+} from the SR leads to hyperthermic seizures. (a) Seizure indices of *DysDf* mutants after being fed various Ca^{2+} channel blockers. The control animals were only fed 5% sucrose and the other drugs were given in a 5% sucrose solution. Statistics were calculated using a one-tailed Mann-Whitney U-test where the following P-values were obtained by comparing to sucrose fed animals: Nifedipine: $P = 0.421$, 2-APB: $P = 0.107$ and Ryanodine: $P = 0.078$. (b) Electrical output from dystrophic heated muscles after being fed overnight with sucrose (control), L-type calcium channel blocker (Nifedipine), Ryanodine SR fast calcium channel blocker or IP_3R SR slow calcium channel blocker (2-APB). 5–6 animals were measured per condition. Seizure onset and subsiding temperatures are noted as well as seizure duration. Animals fed Nifedipine did not show a decrease in seizure activity. Animals fed 2-APB had additional seizure activity that was occurring spontaneously before heating began that was different in its electrical pattern that would be consistent with the observed phenotype of typical *Dys* mutants. This is shown here where output occurs for almost 30 s. This is later followed by a seizure at a reasonable temperature that looks like what would be expected for a dystrophic mutant. This extra output was only seen with animals fed this channel blocker, and in general the occurrence of seizures was less than controls (Supplementary Table 5). Animals fed Ryanodine still had seizures 33% of the time, but in general there was a decrease in the seizure indices associated with these animals, therefore we considered this reagent to have a therapeutic effect. *$P \leq 0.05$, **$P \leq 0.01$, ***$P \leq 0.001$.

These opposing phenotypes are similar to what we report here, where *Dys* mutants have seizures and *Dg* mutants do not. Additionally, *Dys* mutants have an increase in synaptic vesicle docking sites (T-bars) at larval NMJs[23], which could explain our data showing the developmental requirement for Dys. Once the NMJ is established with a normal number of active sites, animals would not be prone to seizures.

Our data also show that Dys and Dg mutants have altered cellular homeostasis. In vertebrates, multiple metabolic disorders have been implicated in seizure activity; for example, mitochondrial encephalopathy, the most common neurometabolic disorder, presents various symptoms including seizures[33] and mice that are partially deficient for mitochondrial superoxide dismutase have an increased incidence of spontaneous seizures[34]. Additionally, *mdx* mice, a model for MD has sustained oxidative stress in skeletal muscle[35–37]. In *Drosophila*, it has been shown that *Dg* mutant larvae have an altered state of cellular homeostasis and are sensitive to ambient temperature. A constant increase in mitochondrial oxidative metabolism, caused by a *Dg* hypomorphic mutation, results in a change in thermoregulatory behavior[38]. In addition, it was reported that suboptimal temperatures and energetic stress accelerate age-dependent muscular dystrophy in both, *Dys* and *Dg* mutants[16]. Now we show that *Dys* and *Dg* mutants have antagonistically abnormal cellular levels of ROS.

ROS are derived from elemental oxygen (O_2), and ROS cascades begin with the superoxide anion radical. Sources for superoxide anion radicals include xanthine oxidase, prostanoid metabolism, catecholamine autooxidation, NAD(P)H oxidase activity and NO synthase. These radicals are generated in normal muscle, and the rate of generation is increased by muscle contraction[39]. In Duchenne MD the absence of dystrophin at the sarcolemma delocalizes and downregulates neuronal nitric oxide synthase (nNOS), which in turn leads to increase in inducible nitric oxide synthase (nNOS) that generates excessive $NO^{\bullet}$[40]. This mechanism can explain extremely high ROS levels in *Dys* mutants. This high level of ROS in dystrophic *Drosophila* can be alleviated by transheterozygous interaction with *Dg* and *Cam,* which indicates a genetic interaction between *Dys* and these two genes in control of cellular homeostasis.

Our study provides the first *in vivo* measurements on dystrophic animals showing that they have hyperthermic seizures that are dependent upon neurotransmission. Dystrophin is required during development, since *Dys* downregulation in adulthood, after muscles and NMJs are already established precludes hyperthermic seizures. Our data suggest that the DGC has a role in signaling at the NMJ: reduction of Dg, a protein that binds Dys[12] and regulates localization of the NMJ specific proteins, prevents dystrophic seizure occurrence. Seizures are associated with abnormal Ca^{2+} release from the SR; introduction of a mutation of Ca^{2+} mediator *Calmodulin* and supply of calcium channel blockers reduce seizures. Taken together, our data show that the DGC acts at the muscle side of the NMJ to regulate muscle cell homeostasis in response to neuronal signaling and implies that Dys is involved in muscle-neuron communication.

Methods

Fly strains and genetics. Fly stocks were maintained at 25°C on a standard cornmeal-agar diet unless otherwise stated. Fly strains used in this study are: *UAS-Dys$^{C\text{-}RNAi}$ (dsDys), tub-Gal4::dsDys/TM6, UAS-Dg^{RNAi} (dsDg), tub-Gal4::dsDg/TM3* (described previously[12] and recombined onto chromosomes with the *tub-Gal4* driver where indicated), loss of function (lof) mutants *DysDf* (deletion of the *Dys* gene generated by outcrossing the deficiency *Df(3R)Exel6184*[41]), *Dg^{O86}/CyO, Dg^{O55}/CyO*[42], *DfKX23/Ser,TM3* (Df(3R)Dl-KX23 - partial deletion of *Dys* gene, Bloomington ID: 2411), *Dys$^{8\text{-}2}$/TM6* (deletion of N-terminal region causing a loss of at least one long isoform[12]), *tub-Gal4/TM3, 24B-Gal4, D42-Gal4, act-Gal4, tub-Gal80^{s}, OregonR*. Alleles used in this study are: *para^{ts1}* (temperature sensitive, lof), *Cam^{n339}* (lof), *mys^{1}* (lof), *cora^{k08713}* (hypomorph), *tkv^{1}* (hypomorph) and *Mad^{12}* (lof). The *RNAi* line directed against *tkv* (*tkv^{RNAi}*) was obtained from the Vienna *Drosophila* RNAi Center. Unless otherwise stated, lines were obtained from Bloomington Stock Center.

Immunohistochemistry. Adult flies were immobilized on a tissue culture dish using Vaseline. The thorax and head were removed and the abdomen was opened in saline buffer (115 mM NaCl, 5 mM KCl, 6 mM $CaCl_2{\bullet}2H_2O$, 1 mM $MgCl_2{\bullet}6H_2O$, 4 mM $NaHCO_3$, 1 mM $NaH_2PO_4{\bullet}1H_2O$, 5 mM trehalose, 75 mM sucrose, and 5 mM N-Tris [hydroxymethyl] methyl-2-aminoethane sulfonic acid). The tissue was then fixed without agitation for 10 minutes at room temperature in 4% formaldehyde. Tissue was fixed for 5 minutes in methanol for the anit-DGluRIIA antibody. Antibody staining was performed as described before[17] except with the use of saline buffer. The following antibodies were used: rabbit anti-Dg[42] (1 : 1000), mouse anti-Dlg (1 : 50; Developmental Studies Hybridoma Bank), mouse anti-DGluRIIA (1 : 50; Developmental Studies Hybridoma Bank), Alexa 488 goat anti-mouse and Alexa 568 goat anti-rabbit (Invitrogen). Samples were then mounted on slides in 70% glycerol, 2% NPG, 1× PBS and analyzed using a confocal microscope (Leica TCS SP5). Quantification of staining intensities was done using Leica software (LAS AF version 2.1.1). The mean pixel value in the area of interest (NMJ) and in the same size area of the background was calculated. The background level was subtracted from the value found in the area of interest. Reported intensities were normalized to control and the Student's t-test was performed for statistical analysis.

Electrophysiology. IFM recordings were done on adult flies raised at 25°C. Flies were 3–5 days old unless otherwise indicated. Platinum electrodes were fashioned via KOH etching. The recording electrode was inserted into the lateral thorax with the ground electrode inserted into the abdomen. Temperature was shifted from room temperature (~25°C) up to ~50°C using an infrared lamp. Signals generated from the IFMs were amplified and digitized with the Micro 1401 data acquisition unit (Cambridge Electronic Design) and analyzed with Spike 2 software (Cambridge Electronic Devices). Temperature was monitored using an analogue thermometer (DKT200, 0–5 V, −20°C−80°C, ±0.3°C, Driesen Kern GmbH) where approximately every ten seconds resulted in a 1°C T increase. Plots were made of voltage output vs. temperature. All plots were scaled the same and converted into binary JPEG images. A macro was written using ImageJ software (NIH) to count the number of pixels of the voltage on the graph during the seizure. When a seizure occurred, a seizure index (S_i) was calculated to reflect the temperature that the seizure started at (T_s), the amplitude of the seizure, and the duration of the seizure. Since the T_s was deemed to be more informative than the size of the seizure, a S_i was calculated by taking the natural logarithm of the pixel count and dividing by the seizure start temperature. This number was then multiplied by 10.

$$\mathbf{S_i} = (\boldsymbol{ln}(\text{pixel number})/\mathbf{T_s}) * \mathbf{10}$$

If no seizure occurred then the index was set to zero because the T_s could not be determined if there was no seizure. Only seizures that occurred at lower than 49°C were considered because at very high temperatures even control animals start having contractions (Fig. 1b).

Statistics. Since our seizure electrophysiological data are not normally distributed, we used non-parametric methods for statistical analysis. Values are reported as M (x/y) where M = median, y = 25th percentile rank and x = 75th percentile rank. For determination of agreement between groups of data, the Kruskal-Wallis test was applied resulting in a chi-squared statistic. For comparison between two data sets a one-tailed Mann-Whitney U-test was used. Graphical representations of data show the median value of the data spread and error bars correspond to the 25th and 75th percentiles. Statistical analysis of muscle degeneration was done using a one-tailed chi-squared test. Statistical analysis of biochemical assays and immunohistochemical signal intensity was done using a one-tailed Student's t-test.

Histology. For analysis of indirect flight muscle (IFM) morphology, 10 μm paraffin-embedded sections were cut from fly thoraxes. In order to prepare *Drosophila* muscle sections, the fly bodies were immobilized in collars in the required orientation and fixed in Carnoy fixative solution (6 : 3 : 1 = Ethanol : Chloroform : Acetic acid) at 4°C overnight. Tissue dehydration and embedding in paraffin was performed as described previously[43]. Histological sections were prepared using a Hyrax M25 (Zeiss) microtome and stained with hematoxylin and eosin. All chemicals for these procedures were obtained from Sigma Aldrich. Muscle analysis was done using a light microscope (Zeiss). The frequency of muscle degeneration was quantified as a ratio of degenerated muscles to the total number of analyzed muscles.

Lipid peroxidation detection. Flies were kept at 29°C for three days after eclosion and emersed in liquid N_2. Cellular extracts were prepared via homogenization of 20–25 whole flies in cell lysis buffer and then boiling the homogenates for 5 min at 100°C followed by centrifuging on high for 5 min. Protein levels in the extracts were determined via the BCA protein assay (Pierce Chemical). 100 μl of fly extract was combined with 300 μl acetic acid (20%, pH 3.5), 300 μl TBA (0.8% w/v in 0.5 M NaOH) and 40 μl SDS (8% w/v). The mixture was heated for 45 min at 100°C to allow for adduct formation. Adducts were then extracted into 1-butanol and the absorption was measured at 540 nm along with appropriate blanks. The raw absorption values minus any absorbance from the blank samples were then normalized to protein content (μg/ml). Three replicates were measured from four or more independent extracts. Data was compared using a one-tailed Student's t-test. Heterozygous animals were the result of crossing mutant stocks to *OregonR*.

Drug assays. Flies (*DysDf* genotype) raised at 25°C that were 3–7 days old were put overnight in vials containing filter paper soaked in 5% sucrose and either 500 μM 2-APB, 20 μM Ryanodine or 3.6 mM Nifedipine. Controls were only kept on sucrose. Electrophysiological measurements of IFMs were done the following day. When testing for drug lethality, *OregonR* wild type flies were used with lethality rates as follows: sucrose (1/10 dead), 2-APB (3/10 dead), Ryanodine (0/10 dead), Nifedipine

(0/10 dead). When testing was conducted on *Dys* mutants there was a much higher lethality rate with both 2-APB and Ryanodine as follows: sucrose (4/15 dead), 2-APB (10/15 dead), Ryanodine (9/15 dead), Nifedipine (1/15 dead).

Reverse transcription quantitative PCR. Quantitative reverse transcription (RT-qPCR) was performed on total RNA derived from whole adult animals. RNAs were extracted from flies with the RNeasy Mini kit (Qiagen), followed by reverse transcription using the High Capacity cDNA Reverse Transcription kit (Applied Biosystems) following the manufacturer's protocols. mRNA amounts were tested with RpL32 as an endogenous control for q-PCR using the Fast SYBR® Green master mix on a Step One Plus 96 well system (Applied Systems). The reactions were incubated at 95°C for 10 min, followed by 40 cycles of 95°C for 15 s and 54°C for 30 s. All reactions were run in triplicate with appropriate blank controls. The threshold cycle (CT) is defined as the fractional cycle number at which the fluorescence passes the fixed threshold. Primers were used as follows: RpL32 forward - AAGATGACCATCCGCCCAGC; RpL32 reverse – GTCGATACCCTTGGGCTTGC; Dg forward – ACTCAAGGACGAGAAGCCGC; Dg reverse – ATGGTGGTGGCACATAATCG; Dys forward – GTTGCAGACACTGACCGACG; Dys reverse - CGAGGGCTCTATGTTGGAGC. The ΔC_T value is determined by subtracting the average RpL32 C_T value from the average Dys/Dg C_T value. The $\Delta\Delta C_T$ value is calculated by subtracting the ΔC_T of the control sample from the ΔC_T of the suspect sample. The relative amount of mRNA is then determined using the expression $2^{-\Delta\Delta CT}$ and the fold reduction is determined using the expression $2^{\Delta\Delta CT}$. Errors for *RNAi* transgenes were determined starting with the standard deviation of the raw C_T values and performing appropriate regression analysis.

1. Barresi, R. & Campbell, K. P. Dystroglycan: from biosynthesis to pathogenesis of human disease. *J Cell Sci* **119**, 199–207 (2006).
2. Grady, R. M. *et al.* Maturation and maintenance of the neuromuscular synapse: genetic evidence for roles of the dystrophin–glycoprotein complex. *Neuron* **25**, 279–293, doi:S0896-6273(00)80894-6 [pii] (2000).
3. Kanagawa, M. & Toda, T. The genetic and molecular basis of muscular dystrophy: roles of cell-matrix linkage in the pathogenesis. *J Hum Genet* **51**, 915–926, doi:10.1007/s10038-006-0056-7 (2006).
4. Sciandra, F. *et al.* Dystroglycan and muscular dystrophies related to the dystrophin-glycoprotein complex. *Ann Ist Super Sanita* **39**, 173–181 (2003).
5. Lim, L. E. & Campbell, K. P. The sarcoglycan complex in limb-girdle muscular dystrophy. *Curr.Opin.Neurol.* **11**, 443–452 (1998).
6. Matsumura, K. & Campbell, K. P. Dystrophin-glycoprotein complex: its role in the molecular pathogenesis of muscular dystrophies. *Muscle Nerve* **17**, 2–15 (1994).
7. Hayashi, Y. K. *et al.* Mutations in the integrin alpha7 gene cause congenital myopathy. *Nat Genet* **19**, 94–97, doi:10.1038/ng0598-94 (1998).
8. Xiong, Y., Zhou, Y. & Jarrett, H. W. Dystrophin glycoprotein complex-associated Gbetagamma subunits activate phosphatidylinositol-3-kinase/Akt signaling in skeletal muscle in a laminin-dependent manner. *J Cell Physiol* **219**, 402–414, doi:10.1002/jcp.21684 (2009).
9. Zhou, Y. W., Thomason, D. B., Gullberg, D. & Jarrett, H. W. Binding of laminin alpha1-chain LG4-5 domain to alpha-dystroglycan causes tyrosine phosphorylation of syntrophin to initiate Rac1 signaling. *Biochemistry* **45**, 2042–2052 (2006).
10. Vandebrouck, A. *et al.* Regulation of capacitative calcium entries by alpha1-syntrophin: association of TRPC1 with dystrophin complex and the PDZ domain of alpha1-syntrophin. *Faseb J* **21**, 608–617 (2007).
11. Sabourin, J. *et al.* Regulation of TRPC1 and TRPC4 cation channels requires an alpha1-syntrophin-dependent complex in skeletal mouse myotubes. *J Biol Chem* **284**, 36248–36261 (2009).
12. Shcherbata, H. R. *et al.* Dissecting muscle and neuronal disorders in a Drosophila model of muscular dystrophy. *EMBO J.* **26**, 481–493 (2007).
13. Greener, M. J. & Roberts, R. G. Conservation of components of the dystrophin complex in Drosophila. *FEBS Lett* **482**, 13–18 (2000).
14. Taghli-Lamallem, O. *et al.* Dystrophin deficiency in Drosophila reduces lifespan and causes a dilated cardiomyopathy phenotype. *Aging Cell* **7**, 237–249 (2008).
15. Allikian, M. J. *et al.* Reduced life span with heart and muscle dysfunction in Drosophila sarcoglycan mutants. *Hum.Mol.Genet.* **16**, 2933–2943 (2007).
16. Kucherenko, M. M., Marrone, A. K., Rishko, V. M., Magliarelli Hde, F. & Shcherbata, H. R. Stress and muscular dystrophy: a genetic screen for dystroglycan and dystrophin interactors in Drosophila identifies cellular stress response components. *Dev Biol* **352**, 228–242 (2011).
17. Klose, M. K., Atwood, H. L. & Robertson, R. M. Hyperthermic preconditioning of presynaptic calcium regulation in Drosophila. *J.Neurophysiol.* **99**, 2420–2430 (2008).
18. Montana, E. S. & Littleton, J. T. Characterization of a hypercontraction-induced myopathy in Drosophila caused by mutations in Mhc. *J.Cell Biol.* **164**, 1045–1054 (2004).
19. Wu, C. F. & Ganetzky, B. Genetic alteration of nerve membrane excitability in temperature-sensitive paralytic mutants of Drosophila melanogaster. *Nature* **286**, 814–816 (1980).
20. Bogdanik, L. *et al.* Muscle dystroglycan organizes the postsynapse and regulates presynaptic neurotransmitter release at the Drosophila neuromuscular junction. *PLoS.One.* **3**, e2084 (2008).
21. Cote, P. D., Moukhles, H. & Carbonetto, S. Dystroglycan is not required for localization of dystrophin, syntrophin, and neuronal nitric-oxide synthase at the sarcolemma but regulates integrin alpha 7B expression and caveolin-3 distribution. *J Biol Chem* **277**, 4672–4679 (2002).
22. Wairkar, Y. P., Fradkin, L. G., Noordermeer, J. N. & DiAntonio, A. Synaptic defects in a Drosophila model of congenital muscular dystrophy. *J Neurosci* **28**, 3781–3789 (2008).
23. van der Plas, M. C. *et al.* Dystrophin is required for appropriate retrograde control of neurotransmitter release at the Drosophila neuromuscular junction. *J.Neurosci.* **26**, 333–344 (2006).
24. Pilgram, G. S., Potikanond, S., van der Plas, M. C., Fradkin, L. G. & Noordermeer, J. N. The RhoGAP crossveinless-c interacts with Dystrophin and is required for synaptic homeostasis at the Drosophila neuromuscular junction. *J Neurosci* **31**, 492–500 (2011).
25. Madhavan, R., Massom, L. R. & Jarrett, H. W. Calmodulin specifically binds three proteins of the dystrophin-glycoprotein complex. *Biochem.Biophys.Res.Commun.* **185**, 753–759 (1992).
26. Heiman, R. G. *et al.* Spontaneous avoidance behavior in Drosophila null for calmodulin expression. *Proc.Natl.Acad.Sci.U.S.A* **93**, 2420–2425 (1996).
27. Deval, E. *et al.* Na(+)/Ca(2+) exchange in human myotubes: intracellular calcium rises in response to external sodium depletion are enhanced in DMD. *Neuromuscul.Disord.* **12**, 665–673 (2002).
28. Surtees, R. Inherited ion channel disorders. *Eur J Pediatr* **159 Suppl 3**, S199–203 (2000).
29. Kushnir, A., Betzenhauser, M. J. & Marks, A. R. Ryanodine receptor studies using genetically engineered mice. *FEBS Lett* **584**, 1956–1965 (2010).
30. Matsumoto, M. *et al.* Ataxia and epileptic seizures in mice lacking type 1 inositol 1,4,5-trisphosphate receptor. *Nature* **379**, 168–171 (1996).
31. Nishimune, H., Sanes, J. R. & Carlson, S. S. A synaptic laminin-calcium channel interaction organizes active zones in motor nerve terminals. *Nature* **432**, 580–587 (2004).
32. Keshishian, H. & Kim, Y. S. Orchestrating development and function: retrograde BMP signaling in the Drosophila nervous system. *Trends Neurosci* **27**, 143–147 (2004).
33. Tucker, E. J., Compton, A. G. & Thorburn, D. R. Recent advances in the genetics of mitochondrial encephalopathies. *Curr Neurol Neurosci Rep* **10**, 277–285 (2010).
34. Liang, L. P. & Patel, M. Mitochondrial oxidative stress and increased seizure susceptibility in Sod2(−/+) mice. *Free Radic Biol Med* **36**, 542–554 (2004).
35. Dudley, R. W. *et al.* Dynamic responses of the glutathione system to acute oxidative stress in dystrophic mouse (mdx) muscles. *Am J Physiol Regul Integr Comp Physiol* **291**, R704–710 (2006).
36. Tidball, J. G. & Wehling-Henricks, M. The role of free radicals in the pathophysiology of muscular dystrophy. *J Appl Physiol* **102**, 1677–1686 (2007).
37. Whitehead, N. P., Pham, C., Gervasio, O. L. & Allen, D. G. N-Acetylcysteine ameliorates skeletal muscle pathophysiology in mdx mice. *J Physiol* **586**, 2003–2014 (2008).
38. Takeuchi, K. *et al.* Changes in temperature preferences and energy homeostasis in dystroglycan mutants. *Science* **323**, 1740–1743 (2009).
39. Reid, M. B. Invited Review: redox modulation of skeletal muscle contraction: what we know and what we don't. *J Appl Physiol* **90**, 724–731 (2001).
40. Bellinger, A. M. *et al.* Hypernitrosylated ryanodine receptor calcium release channels are leaky in dystrophic muscle. *Nat Med* **15**, 325–330 (2009).
41. Christoforou, C. P., Greer, C. E., Challoner, B. R., Charizanos, D. & Ray, R. P. The detached locus encodes Drosophila Dystrophin, which acts with other components of the Dystrophin Associated Protein Complex to influence intercellular signalling in developing wing veins. *Dev Biol* **313**, 519–532 (2008).
42. Deng, W. M. *et al.* Dystroglycan is required for polarizing the epithelial cells and the oocyte in Drosophila. *Development* **130**, 173–184 (2003).
43. Kucherenko, M. M. *et al.* Paraffin-embedded and frozen sections of Drosophila adult muscles. *J Vis Exp*, doi:2438 [pii]10.3791/2438 (2010).

Acknowledgements

We would like to thank H. Ruohola-Baker and R. Ray for fly stocks and reagents, N. Glyvuk, Y. Tsytsyura, G. Vorbrüggen, A. Yatsenko and A. König for comments on the manuscript. This work was funded by Max Planck Society.

Author contributions

AKM designed and performed experiments, analyzed data, wrote the manuscript, MMK performed experiments, analyzed data, RW and MCG helped with electrophysiology and discussed data, HRS designed experiments, analyzed data, wrote the manuscript.

Additional information

Supplementary Information accompanies this paper at http://www.nature.com/scientificreports

Competing financial interests: Authors declare no competing financial interests.

How to cite this article: Marrone, A.K., Kucherenko, M.M., Wiek, R., Göpfert, M.C. & Shcherbata, H.R. Hyperthermic seizures and aberrant cellular homeostasis in *Drosophila* dystrophic muscles. *Sci. Rep.* **1**, 47; DOI:10.1038/srep00047 (2011).